

## Article

# Toward Probing Surface Magnetism with Highly Charged Ions

Perla Dergham <sup>1,\*</sup>, Friedrich Aumayr <sup>2</sup>, Emily Lamour <sup>1</sup>, Stéphane Macé <sup>1</sup>, Christophe Prigent <sup>1</sup>, Sébastien Steydli <sup>1</sup>, Dominique Vernhet <sup>1</sup>, Matthias Werl <sup>2</sup>, Richard Arthur Wilhelm <sup>2</sup> and Martino Trassinelli <sup>1,\*</sup>

<sup>1</sup> Institut des NanoSciences de Paris (INSP), Sorbonne Université, CNRS UMR 7588, 75005 Paris, France

<sup>2</sup> Institute of Applied Physics, TU Wien, 1040 Vienna, Austria

\* Correspondence: dergham@insp.jussieu.fr (P.D.); martino.trassinelli@insp.jussieu.fr (M.T.)

**Abstract:** X-rays produced during collisions between Highly Charged Ions (HCI) and sample surfaces can potentially be used to investigate the surface's magnetic properties, taking advantage of the (partial) conservation of the spin of the electrons captured by the ion during the collision. We conducted studies to characterize the X-ray detection system and to determine, with a sub-degree accuracy, the incident angle between the incoming ions and the sample surfaces. A series of proof-of-principle experiments are presented involving an Ar<sup>17+</sup> ion beam interacting with a nonmagnetic Si sample. The obtained X-ray spectra show a significant dependency in terms of X-ray yield and energy on the ion incidence angle. These findings will be used to guide future ion–magnetic surface studies.

**Keywords:** highly charged ion; ion-surface collision; magnetic properties; X-ray detection



**Citation:** Dergham, P.; Aumayr, F.; Lamour, E.; Macé, S.; Prigent, C.; Steydli, S.; Vernhet, D.; Werl, M.; Wilhelm, R.A.; Trassinelli, M. Toward Probing Surface Magnetism with Highly Charged Ions. *Atoms* **2022**, *10*, 151. <https://doi.org/10.3390/atoms10040151>

Academic Editors: Izumi Murakami, Daiji Kato, Hiroyuki A. Sakaue and Hajime Tanuma

Received: 31 October 2022

Accepted: 8 December 2022

Published: 13 December 2022

**Publisher's Note:** MDPI stays neutral with regard to jurisdictional claims in published maps and institutional affiliations.



**Copyright:** © 2022 by the authors. Licensee MDPI, Basel, Switzerland. This article is an open access article distributed under the terms and conditions of the Creative Commons Attribution (CC BY) license (<https://creativecommons.org/licenses/by/4.0/>).

## 1. Introduction and Scientific Context

Surface properties present unexpected features in comparison with those of the bulk, and are fascinating to study, particularly with the most recent technological advancements in magnetic 2D materials. A promising method for investigating surface properties involves using highly charged ions (HCI) [1,2]. When an HCI comes close enough to the surface of a sample (a few angstroms above the surface), the Coulomb potential barrier between the ions and the surface is lowered to the Fermi level of the target, and electron capture occurs. The electrons are resonantly transferred from the surface and occupy highly excited states of the ion [3]. The process is so fast (in the order of 10 fs) that the ion is almost or entirely neutralized above the surface without refilling the innermost shells, forming a hollow atom [4]. Here, the purpose is to investigate the possibilities of probing the surface properties of magnetic samples from their interactions with HCIs.

In general, the relaxation of a hollow atom involves multiple processes, including radiative and Auger processes, as well as interatomic Coulombic decay (ICD) [5]. The non-radiative processes dominate at the earliest phases of the deexcitation cascade whereas the radiative process takes over in the last steps, where ions relax by emitting photons. Due to the selective population of states with different total spin  $S$ , information on the magnetic states of a surface can be extracted from the Auger electrons or from the energy of the emitted X-rays. The spin is mainly conserved in radiative decay due to the electric dipole selection rule. In the Auger decay, the spin is partially conserved due to the ejection of minority spin electrons visible in the calculation of matrix elements that disfavors the interaction of electrons with the same spin direction [6]. On the contrary, ICD does not conserve the total spin numbers, thereby drowning out the information on the initial electron polarization. However, its contribution can be minimized using grazing angle collisions. More precisely, the grazing angle must not exceed a critical angle to prevent the ions from penetrating the bulk and hence limiting the ion beam interaction to the surface atoms only. The value of the critical angle is given in Section 3.1 for our case study.

The ability to detect the presence of a ferromagnetic ordered phase in an ion–surface interaction was demonstrated in the past using Auger spectroscopy [7,8]. In these first attempts, only qualitative evidence was obtained, and a dispute arose in the scientific community on the general applicability of this method [9]. Our goal is to detect surface magnetism via X-ray emission. When the last steps of the decay cascade are considered, the capture by the ion of polarized or non-polarized electrons from the surface induces different populations of the L-shell, as shown in Figure 1a,b. The L-shell can thus be filled from one to eight electrons for the paramagnetic phase and only from one to four electrons for the ferromagnetic phase due to the Pauli exclusion principle in the ideal case without any loss of spin polarization. Therefore, a shift in the transition energies  $KL^x \rightarrow K^2L^{x-1}$  is expected when ferromagnetic domains are present at the surface due to the lower screening effect of the partially filled L-shell. For example, for  $\text{Ar}^{17+}$  ions hitting a Ni sample, a maximum shift of 177 eV of the ~3 keV transition is expected between the case of single electron capture and a full ion neutralization. Considering a (uniform) population of 1–8 or 1–4 electrons of the L-shell for paramagnetic and ferromagnetic phases, respectively, the expected shift is reduced to 36 eV. For these estimations, we considered the  $K_{\alpha}$  X-ray energy of neutral argon and the  $1s2s^p2p^q - 1s^22s^p2p^{q-1}$  transition energies and yields from Ref. [10]. Before studying HCIs interacting with magnetic surfaces, a series of proof-of-principle investigations are required. Such an investigation is the object of the present article.

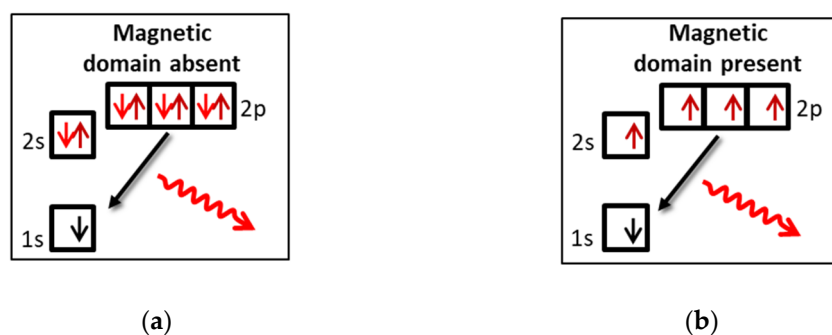


**Figure 1.** Radiative Deexcitation (a) in the absence of magnetic domains with a fully occupied L-shell and (b) in the presence of magnetic domains with a half occupied L-shell.

The following section describes the setup and installation of our ion-surface experiment. It is followed by a section dedicated to the characterization of a new silicon drift detector for X-ray detection. In the final section, we present results obtained with a non-magnetic Si sample.

## 2. Setup and Installation

### 2.1. Ion Source and Beamline

The SIMPA (French acronym for multicharged ion source of Paris) facility [11] is an installation that allows the production of highly charged positive ions to study ion-matter interactions. It is divided into two main parts: an Electron-Cyclotron Resonance Ion Source (ECRIS) and a beamline. The ECRIS generates highly charged ions with energies of several q keV (with q indicating the charge of the ion), such as  $\text{Ne}^{10+}$ ,  $\text{Ne}^{9+}$ ,  $\text{Ar}^{16+}$ , and  $\text{Ar}^{17+}$  that are charge-over-mass selected by a magnetic dipole. The selected ion beam is transported through the beamline equipped with a series of Faraday cups, quadrupoles, and steerers to monitor and shape it before entering the collision chamber. In the present paper, we exhibit results obtained with an ion beam of  $\text{Ar}^{17+}$  ions at 170 keV with an intensity in the order of nA (true charge current) on the sample.

### 2.2. Sample Preparation and Interaction Chamber

To conduct an ion-surface experiment on a given sample, it is necessary to be aware of its chemical composition. Most importantly, we must ensure that no external contaminant

atoms stick to the surface. Therefore, the sample is sputter cleaned using a low energy  $\text{Ar}^+$  ion beam to remove the surface atom, including the contaminants. After the soft ion bombardment, the sample is flash-annealed at a high temperature ( $\sim 600^\circ\text{C}$ ) in order to rearrange the atoms on the surface. After these treatments, Auger electron spectroscopy (AES) is performed to check the composition of the sample surface [12]. After ensuring that our surface is clean, the sample is transferred into the interaction chamber to interact with the HCl beam. To keep the sample surface clean, both chambers are under ultra-high vacuum conditions, with typical pressures of  $10^{-9}$  and  $10^{-10}$  mbar, for the interaction and preparation chambers, respectively.

The interaction chamber is equipped with a 6-axis goniometer that allows us to rotate and translate the sample. A heater is located beneath the sample holder, allowing the sample temperature to vary. Indeed, for specific samples, different magnetic phases are induced by varying the temperature. The rotation presents an accuracy of  $0.05^\circ$ , allowing an accurate setting for the grazing collision conditions. In the case of an  $\text{Ar}^{17+}$  beam at 170 keV impacting Ni and Si samples, this accuracy makes it possible to position the samples below the theoretical critical angles for complete specular reflection of the projectiles from such surfaces following Ref. [13]. Their values are  $\varnothing_{crit} = 3.23^\circ$  for a Ni sample and  $\varnothing_{crit} = 1.56\text{--}2.06^\circ$  for a Si one.

### 2.3. X-ray Detector Characterization

Measuring the emitted X-rays by the ions during the ion–surface collision in terms of energy and yield requires the use of a well characterized detection system. We opt for a new polymer window silicon drift detector SiriusSD, from RAYSPEC (Buckinghamshire, United Kingdom). To characterize it in terms of resolution and absolute efficiency, we compare its performance with respect to two well-characterized reference silicon drift detectors [14]. The experiment consists of bombarding various solid targets with a 10 keV electron beam, producing fluorescence X-rays of different energies [15]. The targets allow us to cover a wide energy range from a few hundred eV to approximately 9 keV. Using the X-ray peaks and the already-known efficiency of the reference detectors, SiriusSD’s efficiency and resolution have been extracted. The characterization experiment reveals that the SiriusSD has an efficiency of about 75% at 3 keV and beyond. In the low energy range, the SiriusSD surpasses the reference detectors with an efficiency of 40% for  $500 \text{ eV} < E < 1 \text{ keV}$ . The extraction of the efficiency will be presented in a detailed forthcoming paper. Moreover, the SiriusSD presents a remarkable resolution that goes from 60 eV at 200 eV to 160 eV at 9 keV (see Figure 2). At 3 keV, the resolution is about 100 eV which is only three times larger than the expected shift for  $\text{Ar}^{17+}$  ions hitting a full polarized sample (estimated to be about 36 eV). This promising feature makes the measurement of tiny energy shifts induced by different magnetic phases of the sample surface possible.

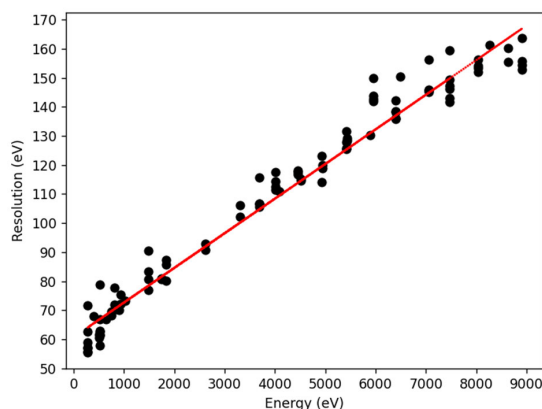


**Figure 2.** Experimental Determination of the SiriusSD Detector Resolution as a Function of the Photon Energy. The Dispersion of the Data is Mainly Caused by the Use of Different Targets that Induce Different Level of Background and the Possible Presence of Partially Resolved Lines.

### 3. Preliminary Results with a Si Target

A preliminary ion-surface investigation has been conducted using a Si one-inch wafer as a sample. We chose Si for preliminary tests since numerous teams have extensively studied it in the past.

#### 3.1. Determination of the Incident Angles Using X-ray Yield

The difficulty in ion–surface experiments at a grazing angle lies in determining the real zero angle between the sample and the incoming ions. Our procedure is to rotate the silicon target with respect to the ion beamline reference axis from high angles (typically  $45^\circ$ ) to low ones and to measure for each “read” angle ( $\theta_{read}$ ) the emitted X-ray yields at  $\sim 3$  keV. To limit the area covered by the detector, a collimator (10 mm in diameter and 80 mm in length) pointing towards the target’s center was placed in front of SiriusSD. As illustrated in Figure 3, the X-ray yield decreases as the angle decreases. A biquadratic polynomial is used to fit the acquired values in this preliminary study, although a  $\sin(\theta - \theta_{read})$  works better for small angles, but this does not significantly change the final results. We find that the target-beam zero angle (the real angle) is at  $\theta_{read} = -8.0 \pm 0.5^\circ$ . Consequently,  $\theta_{read} = -8^\circ$  corresponds to  $\theta_{real} = 0^\circ$ , and  $\theta_{read} = 45^\circ$  to  $\theta_{real} = 53^\circ$ . This curve and, consequently, the real angle deduced from it strongly depends on the ion beam characteristics (emittance, and main propagation axis of the ion beam). These characteristics are defined by the ion beam preparation. It is then essential to repeat this scan as soon as the ion beam conditions change.

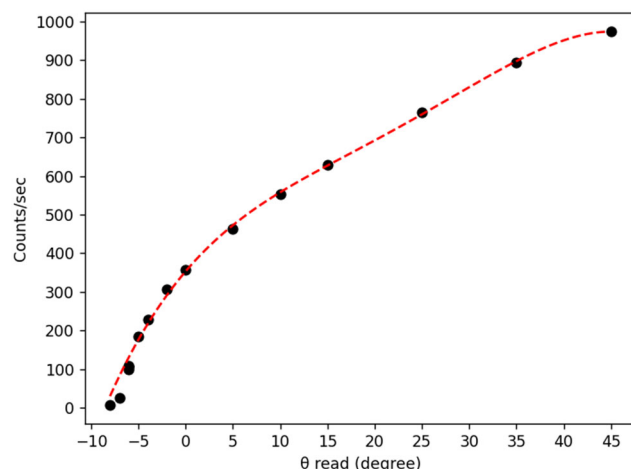


**Figure 3.** Detected counts per second for  $\text{Ar}^{17+}$  at 170 keV colliding with a Si sample at various incidence angles.

#### 3.2. X-ray Spectra Dependency on the Incidence Angle

In Figure 4a, we present two X-ray spectra recorded when an  $\text{Ar}^{17+}$  beam hits the Si sample at two different real angles. As we can see, when the angle decreases, the dominant peak (transitions from  $n \geq 2 \rightarrow n = 1$ ) shifts to higher energy while the remaining portion of the spectrum changes drastically. These features indicate the ion’s excited levels’ populations that differ in ion–solid and ion–surface conditions. This results in a varied screening effect and a different energy of the emitted X-rays. For high angles, such as  $53^\circ$ , the ion captures many electrons which gives rise to the fact that the L-shell is quickly filled up, resulting in a high screening effect while decaying the K-shell. Consequently, a “low” photon energy is measured. On the other hand, for grazing incidence reached at  $2^\circ$ , much fewer electrons are captured, the L-shell is less filled up, and hence the emitted X-ray photon energy is higher. This behavior is in agreement with previous works [16].

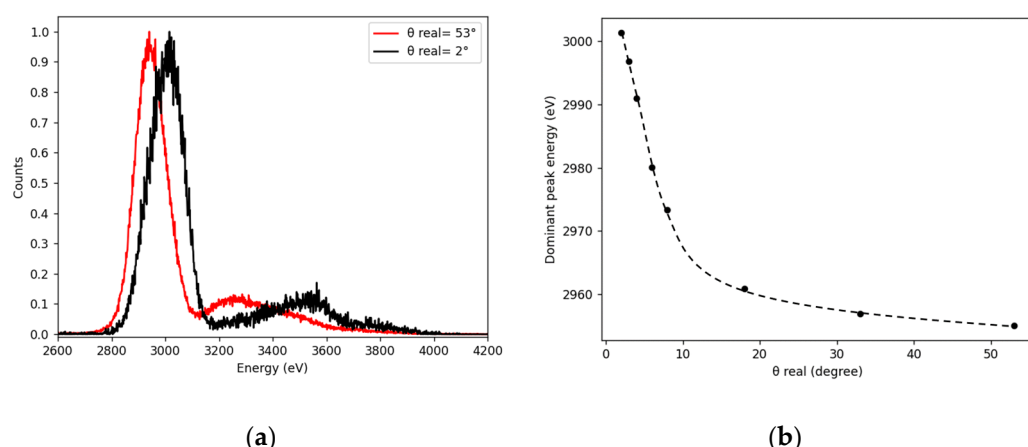


**Figure 4.** (a) X-ray spectra of  $\text{Ar}^{17+}$  at 170 keV hitting a Si sample at real angles of  $53^\circ$  and  $2^\circ$ ; (b)  $K_\alpha$  barycenter shift with respect to the angle.

More quantitatively, the barycenter position of the  $K_\alpha$  transition ( $n = 2 \rightarrow n = 1$ ) is measured with respect to the real angle. The resulting shift between  $53^\circ$  and  $2^\circ$  is evaluated to be  $46 \pm 1$  eV, illustrating that we are very sensitive to a tiny variation of the photon energy and subsequently to the L-shell population. For future experiments, we plan on measuring changes in the X-ray spectra and the barycenter positions at a fixed incidence angle (less than the critical angle) while varying a sample's temperature, thus altering their magnetic phase and consequently the filling of the L shell (see Section 1).

#### 4. Conclusions

To summarize, we present our setup for investigating the first atomic layers of magnetic samples in ion-surface experiments using low-resolution X-ray spectroscopy. For this purpose, the characterization of a new solid-state detector equipped with a polymer window and the first proof-of-principle experiments with a nonmagnetic sample are reported. The resolution of the silicon drift detector is remarkable: a value of 100 eV at 3 keV is found, enabling the measurement of a shift in the energy of the X-ray transition emitted by the ion when ferro/para magnetic phases are present. Furthermore, we demonstrate the possibility of determining the real angle between the sample and the ion beam by measuring the emitted X-ray yield under various angles of our goniometer. With an accuracy of about  $0.5^\circ$ , this is enough to set the grazing angle below the predicted critical angle. In addition, we carry out a series of preliminary experiments with a nonmagnetic Si sample bombarded by a 170 keV  $\text{Ar}^{17+}$  beam to visualize the change of the  $\sim 3$  keV transition position when varying the collision conditions from an ion-bulk interaction to an ion-surface one. A shift of 46 eV is found with a sensitivity of about 1 eV or better. This finding will be utilized as a reference for forthcoming ion-magnetic surface experiments.

**Author Contributions:** Conceptualization, M.T.; Data curation, P.D.; Funding acquisition, P.D., F.A., E.L., C.P., D.V., R.A.W. and M.T.; Investigation, P.D., E.L., C.P. and M.T.; Methodology, P.D., E.L., C.P. and M.T.; Project administration, M.T.; Resources, S.M. and S.S.; Writing—Original draft, P.D., E.L., C.P. and M.T.; Writing—Review & editing, F.A., D.V., M.W. and R.A.W. All authors have read and agreed to the published version of the manuscript.

**Funding:** The doctoral contract of Perla Dergham is funded by Sorbonne Université. The authors acknowledge the support of the French Agence Nationale de la Recherche (ANR) under reference ANR-20-CE91-0007 and the Austrian Fonds zur Förderung der wissenschaftlichen Forschung (FWF) under project No. I 4914-N (project DIMAS).

**Data Availability Statement:** Not applicable.

**Conflicts of Interest:** The authors declare no conflict of interest.

## References

1. Arnau, A.; Aumayr, F.; Echenique, P.; Grether, M.; Heiland, W.; Limburg, J.; Morgenstern, R.; Roncin, P.; Schippers, S.; Schuch, R.; et al. Interaction of slow multicharged ions with solid surfaces. *Surf. Sci. Rep.* **1997**, *27*, 113–239. [[CrossRef](#)]
2. Schneider, D.H.G.; Briere, M.A. Investigations of the interactions of highest charge state ions with surfaces. *Phys. Scr.* **1996**, *53*, 228. [[CrossRef](#)]
3. Winter, H.; Aumayr, F. Hollow atoms. *J. Phys. B At. Mol. Opt. Phys.* **1999**, *32*, R39. [[CrossRef](#)]
4. Briand, J.P.; De Billy, L.; Charles, P.; Essabaa, S.; Briand, P.; Geller, R.; Desclaux, J.P.; Bliman, S.; Ristori, C. Production of hollow atoms by the excitation of highly charged ions in Interaction with a metallic surface. *Phys. Rev. Lett.* **1990**, *65*, 159. [[CrossRef](#)] [[PubMed](#)]
5. Wilhelm, R.A.; Gruber, E.; Schwestka, J.; Kozubek, R.; Madeira, T.I.; Marques, J.P.; Kobus, J.; Krasheninnikov, A.V.; Schleberger, M.; Aumayr, F. Interatomic coulombic decay: The mechanism for rapid deexcitation of hollow atoms. *Phys. Rev. Lett.* **2017**, *119*, 103401. [[CrossRef](#)] [[PubMed](#)]
6. Madesis, I.; Laoutaris, A.; Zouros, T.J.M.; Benis, E.P.; Gao, J.W.; Dubois, A. Pauli Shielding and Breakdown of Spin Statistics in Multielectron Multi-Open-Shell Dynamical Atomic Systems. *Phys. Rev. Lett.* **2020**, *124*, 113401. [[CrossRef](#)] [[PubMed](#)]
7. Unipan, M.; Robin, A.; Winters, D.F.A.; Morgenstern, R.; Hoekstra, R. Probing local spin ordering at surfaces by  $\text{He}^{2+}$  ions. *Phys. Rev. A* **2006**, *74*, 062901. [[CrossRef](#)]
8. Unipan, M.; Robin, A.; Morgenstern, R.; Hoekstra, R. Local spin polarization at surfaces probed by hollow atoms. *Phys. Rev. Lett.* **2006**, *96*, 177601. [[CrossRef](#)] [[PubMed](#)]
9. Busch, M.; Wethekam, S.; Winter, H. Reexamination of local spin polarization at surfaces probed by hollow atoms. *Phys. Rev. A* **2008**, *78*, 010901. [[CrossRef](#)]
10. Bhalla, C.P. K-shell auger rates, transition energies, and fluorescence yields of variously ionized states of argon. *Phys. Rev. A* **1973**, *8*, 2877. [[CrossRef](#)]
11. Gumberidze, A.; Trassinelli, M.; Adrouche, N.; Szabo, C.I.; Indelicato, P.; Haranger, F.; Isac, J.M.; Lamour, E.; Le Bigot, E.O.; Mérot, J.; et al. Electronic temperatures, densities, and plasma X-ray emission of a 14.5 GHz electron-cyclotron resonance ion source. *Rev. Sci. Instrum.* **2010**, *81*, 033303. [[CrossRef](#)] [[PubMed](#)]
12. Dahman, Y. *Nanotechnology and Functional Materials for Engineers*; Elsevier: Amsterdam, The Netherlands, 2017; pp. 39–41.
13. Winter, H. Collisions of atoms and ions with surfaces under grazing incidence. *Phys. Rep.* **2002**, *367*, 387–582. [[CrossRef](#)]
14. Lamour, E.; Prigent, C.; Eberhardt, B.; Rozet, J.P.; Vernhet, D. 2E1  $\text{Ar}^{17+}$  decay and conventional radioactive sources to determine efficiency of semiconductor detectors. *Rev. Sci. Instrum.* **2009**, *80*, 023103. [[CrossRef](#)] [[PubMed](#)]
15. Winick, H. *X-ray Data Booklet*; Lawrence Berkeley National Laboratory: Oakland, CA, USA, 2001.
16. d'Etat, B.; Briand, J.P.; Ban, G.; de Billy, L.; Desclaux, J.P.; Briand, P. Interaction of  $\text{Ar}^{17+}$  ions on metallic surfaces at grazing incidence. *Phys. Rev. A* **1993**, *48*, 1098. [[CrossRef](#)] [[PubMed](#)]